



Influence of layer separation on the determination of stomach smooth muscle properties

Mischa Borsdorf¹ · Markus Böl² · Tobias Siebert¹

Received: 2 February 2021 / Revised: 1 April 2021 / Accepted: 14 April 2021 / Published online: 26 April 2021
© The Author(s) 2021

Abstract

Uniaxial tensile experiments are a standard method to determine the contractile properties of smooth muscles. Smooth muscle strips from organs of the urogenital and gastrointestinal tract contain multiple muscle layers with different muscle fiber orientations, which are frequently not separated for the experiments. During strip activation, these muscle fibers contract in deviant orientations from the force-measuring axis, affecting the biomechanical characteristics of the tissue strips. This study aimed to investigate the influence of muscle layer separation on the determination of smooth muscle properties. Smooth muscle strips, consisting of longitudinal and circumferential muscle layers (whole-muscle strips [WMS]), and smooth muscle strips, consisting of only the circumferential muscle layer (separated layer strips [SLS]), have been prepared from the fundus of the porcine stomach. Strips were mounted with muscle fibers of the circumferential layer inline with the force-measuring axis of the uniaxial testing setup. The force–length (FLR) and force–velocity relationships (FVR) were determined through a series of isometric and isotonic contractions, respectively. Muscle layer separation revealed no changes in the FLR. However, the SLS exhibited a higher maximal shortening velocity and a lower curvature factor than WMS. During WMS activation, the transversally oriented muscle fibers of the longitudinal layer shortened, resulting in a narrowing of this layer. Expecting volume constancy of muscle tissue, this narrowing leads to a lengthening of the longitudinal layer, which counteracted the shortening of the circumferential layer during isotonic contractions. Consequently, the shortening velocities of the WMS were decreased significantly. This effect was stronger at high shortening velocities.

Keywords Contractile muscle properties · Uniaxial tensile experiments · Force–velocity relationship · Force–length relationship · Stomach · Separated muscle layer · Organ wall

Introduction

There are three types of muscles: skeletal, cardiac, and smooth muscles. The latter are predominantly located in the walls of blood vessels and organs of the gastrointestinal, urogenital, and respiratory tract. Smooth muscles are non-striated and cannot be controlled voluntarily. Through complex coordination between contraction and relaxation,

they facilitate the propulsion of various contents within the body and regulate the inner pressure of organs. Due to their distinct features and crucial role in the healthy functioning of various vital body systems, research on smooth muscles has been of high physiological and medical interest [1, 53].

Typically, walls of hollow organs consist (from inside to outside) of mucosal, muscular, and serosal layers. A decisive aspect of the study of smooth muscles are active biomechanical properties, including the characteristic force–length relationship (FLR) [15] and the hyperbolic force–velocity relationship (FVR) [20]. Their examination yields experimental data, which are necessary for the development of muscle models [46] and realistic three-dimensional models of organs [23, 42]. These, in turn, can describe the organ in health and disease and advance the knowledge and treatment of various medical conditions.

Active biomechanical properties of muscles are commonly examined through in vitro uniaxial tensile

This article is part of the Topical Collection on Muscle physiology

✉ Mischa Borsdorf
mischa.borsdorf@inspo.uni-stuttgart.de

¹ Department of Motion and Exercise Science, University of Stuttgart, Stuttgart, Germany

² Institute of Mechanics and Adaptronics, Department of Mechanical Engineering, Braunschweig University of Technology, Braunschweig, Germany

experiments [43, 50], in which muscle forces are measured in one direction only. Typically, muscle tissue is mounted along the muscle direction to a force-measuring device, while muscle activation is initiated through electrical or pharmacological stimulation. Thereby, biomechanical properties of smooth muscles in uniaxial experiments have been examined on tissue specimens, dissected from the bladder [8, 17, 25, 28, 30, 32, 38, 39, 42, 45, 54–58], the stomach [18, 23, 34, 49], the intestine [2, 3, 13, 16, 26, 29, 31], the trachea [7, 35, 47, 48, 51], or from blood vessels [11, 12, 19, 36, 37, 60].

However, the walls of the urinal and gastrointestinal organs contain multiple smooth muscle layers with different muscle fiber orientations [6, 33, 41]. While various studies conducted tests on isolated muscle layers [4, 51, 54], muscle bundles [28, 32, 38, 56], or single smooth muscle cells [18], active biomechanical properties are frequently investigated of strips from which the muscle layers are not separated [8, 16, 30, 34, 49, 58]. In such experiments, narrow strips are cut and mounted so that the examined muscle layer and specifically their muscle fibers are aligned lengthwise to the force-measuring axis of the measuring device. In contrast, the other muscle layers (with deviating muscle fiber directions) are still attached. Therefore, strip activations initiate muscle contractions in more directions than just in the lengthwise axis of the strip. Since the strips are not fixed transversally, this would cause a shortening in that direction. Although generally neglected, a transverse shortening may have a considerable effect on examining biomechanical properties through uniaxial experiments. To date, there has not been a systematic study that investigated the influence of layer separation on the determined muscle properties.

The aim of this study is to examine the influence of muscle layer separation on the determined muscle properties. Therefore, we investigated the active biomechanical properties of smooth muscle strips, consisting of the whole-muscle tissue, and muscle strips, consisting of only one separated muscle layer. Strips were dissected from the ventral fundus of the pig stomach, as this region exhibits two orthogonally oriented, distinct muscle layers [6, 49]. Uniaxial experiments were conducted to investigate muscle properties, including the FLR and FVR.

Materials and methods

Experimental setup

Porcine stomachs of healthy domestic pigs (*Sus scrofa domestica*, age ≈ 6 month, mass ≈ 100 kg) were obtained from a slaughterhouse immediately after animal sacrifice. After the death of the animal, stomachs were prepared within 90 min. The experiments were conducted on overall

nineteen ($n = 19$) gastric smooth muscle strips cut from 12 healthy pig stomachs. The experimental setup, handling, and preparation of gastric smooth muscle tissue have been described earlier in detail [23, 49]. An aerated (95% O₂ and 5% CO₂) Krebs solution (124 mM NaCl; 5 mM KCl; 2.5 mM CaCl₂; 15 mM NaHCO₃; 1.2 mM KH₂PO₄; 1.2 mM MgSO₄; 10 mM C₆H₁₂O₆; pH 7.3 at 37 °C) was used for storage of the tissue and realization of the experiments at temperatures of 4 °C and 37 °C, respectively. To eliminate spontaneous contractions, the method of adding 50 μ M methylene blue to the solution plus illumination was used during experiments [10, 24, 40]. Smooth muscle tissue strips (0.26 ± 0.11 g) of 15×7 mm were dissected from the ventral fundus in the circumferential direction (i.e., transversal to the direction of the gastric serosal folds and orthogonal to the greater curvature, see Fig. 1a). Experiments were performed on strips from which only the mucosal layer was removed (whole-muscle strips, WMS), and strips from which the mucosal and the longitudinal muscle layers were removed, leaving only the circumferential smooth muscle layer (separated layer strips, SLS). Both ends of the strip were threaded into small rectangular blocks ($10 \times 8 \times 3$ mm) with a braided fishing line. Via these blocks, the strip was mounted vertically to a dual-mode muscle lever system (Aurora Scientific 305C-LR; accuracy: ± 1 mN in force; ± 1 μ m in length), to be part of the Aurora Scientific 805A in vitro muscle apparatus. The circumferential layer was aligned along the force-measuring axis e_{circ} (Fig. 1b, c). After the strips were suspended in a relaxed state at a very short length (clearly sagging), they were passively stretched via an isokinetic ramp (5 mm/min) until a passive force of 1–3 mN was reached. After reaching the end of the ramp, the strips were kept at this length, while the passive force development settled to a negligible initial value (< 1 mN). The length of the strips, averaging 10.8 ± 1.3 mm between attachment threads, was determined with a digital sliding caliper (± 0.02 mm accuracy) and was defined as slack length (L_S). Muscle contractions were induced by supramaximal electrical stimulations (1000 mA, 100 Hz, 5 ms) for 16 s. The muscle properties were determined after an equilibration period of 30 min [8, 23, 49].

Determination of muscle properties

Uniaxial experiments were performed in vitro on nineteen ($n = 19$) tissue strips. Table 1 summarizes the number of samples examined for each analyzed parameter. The FLR was investigated by a series of isometric contractions with length increments of 20% L_S until a decrease in force, and hence the descending limb of the FLR, was established. The muscle length at maximum isometric force (F_{im}) was defined as the optimum muscle length (L_0). The ascending and descending limbs of the FLR were fitted using linear regression models ($f(x) = mx + b$, with $x = L/L_S$) to

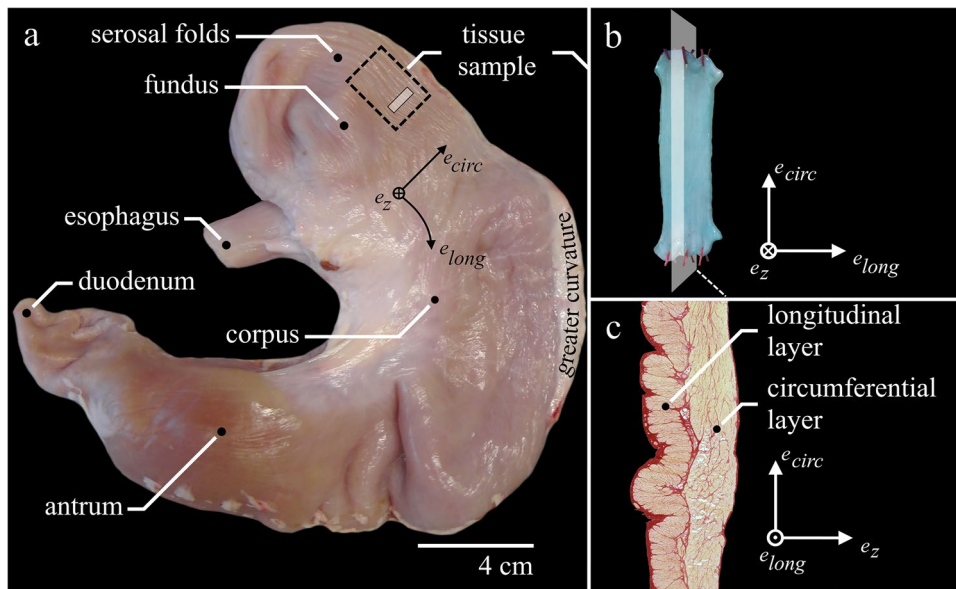


Fig. 1 Tissue strip structure and location in the porcine stomach. **a** Ventral view of a porcine stomach with anatomical regions. The dashed black rectangle indicates the location from which tissue strips were dissected. The visible gastric serosal folds run inline with the greater curvature. **b** Tissue strip, mounted in the uniaxial tensile experiments. Note the blue color of the strip was due to the addition

of methylene blue to the solution. The transparent white plane illustrates the **c** lengthwise histological cut of a porcine muscle tissue strip from the fundus. The mucosal layer is missing, as it was cut away for the experiments. The thin serosal layer on the outside (left), the outer longitudinal and the inner circumferential muscle layers can be identified

extrapolate to lengths of zero force generation [36, 60]. The respective distances to L_0 were defined as the width of the ascending (w_{asc}) and descending (w_{desc}) limbs.

Before determining the FVR, the strips were stimulated isometrically every 5 min until a stable maximal isometric force generation (deviation $< 3\% F_{im}$) was established.

Table 1 The number of investigated tissue samples of each strip group for the determined muscle properties and parameters. FLR parameters: L_0 , w_{asc} , w_{desc} , p_{act} , and p_{pass} . FVR parameters: v_{max} and $curv$

Stomach Number	Whole-muscle strips		Separated layer strips	
	FLR	FVR	FLR	FVR
1	X		X	X
2			X	X
3	X	X	X	
4	X		X	X
5	X	X		
6	X	X	X	X
7	X	X	X	X
8	X		X	
9			X	X
10	X	X		
11	X	X	X	X
12	X	X		
Number of Samples	10	7	9	7

A series of 6 isotonic contractions determined the FVR at L_0 against forces of $0.1\text{--}0.9 F_{im}$. The data were fitted with Hill’s hyperbolic equation to yield the maximum shortening velocity (v_{max}) and the curvature factor $curv = a/F_{im}$ (a describes the force asymptote). Between all contractions, recovery phases of 5 min were interposed, and the “cycling-protocol” by Brenner [9] was applied.

The cross-sectional area (CSA) of the strip at L_0 was determined from the strip volume and the length of the tissue between the stitches. The volume was calculated by its wet weight, assuming a density of 1.05 g/cm^3 [19]. F_{im} and the passive isometric force were divided by the strip’s CSA to calculate the maximum active stress (p_{act}) and the corresponding passive stress at L_0 (p_{pass}), respectively.

Histological observations

Histological analyses were performed exemplarily for one WMS strip to show typical stomach smooth muscle structure. Cross-sectional, lengthwise-sectional, and in-plane slices were stained with Picrosirius Red staining protocol [33], exhibiting two distinct muscle layers. The outer muscle layer contains muscle fibers, oriented in the longitudinal direction, whereas the inner muscle layer consists of muscle fibers in the circumferential direction. The procedure is described in detail in previous studies [6, 30, 49].

Statistics

For statistical analyses, muscle properties were normalized as follows: (1) Force and length values were divided by individual CSA and L_0 , respectively. (2) Velocity data were normalized to optimal muscle length and expressed in L_0/s . The strips were differentiated according to their composition (WMS vs. SLS). The biomechanical properties were analyzed using seven parameters (L_0 , w_{asc} , w_{desc} , p_{act} , p_{pass} , v_{max} , and $curv$). No indication for deviation from normal distribution was found using the Kolmogorov–Smirnov test with $p > 0.05$. Each parameter was tested for significant differences using Student's unpaired t-test. A significance level of $p < 0.05$ was used for all analyses. Statistical analyses were carried out using MATLAB (The Mathworks, Inc., Natick, MA, USA).

Results

The FLR and FVR of whole-muscle strips and separated layer strips are shown in Fig. 2. The shape of the mean active isometric FLR was similar for both groups investigated (Fig. 2a). Specifically, the FLR exhibited a linear ascending limb, a bell-shaped plateau region, and a linear descending limb. No differences have been found for optimum muscle length (WMS: $L_0 = 2.86 \pm 0.23 L/L_S$, SLS: $L_0 = 2.98 \pm 0.43 L/L_S$). Furthermore, there were no differences in w_{asc} and w_{desc} between both groups of strips (Table 2). However, p_{act} was significantly lower for WMS (58.5 ± 11.5 kPa) compared to SLS (160.9 ± 66.5 kPa) (Fig. 3a).

The FVR was normalized to F_{im} and v_{max} in Fig. 2b. Both groups of strips exhibited a typical hyperbolic shape of the FVR. Maximum shortening velocity was lower ($p = 0.0025$, Fig. 3b) for WMS ($v_{max} = 0.023 \pm 0.005 L_0/s$) compared to SLS ($v_{max} = 0.042 \pm 0.012 L_0/s$). Furthermore, curvature factor of WMS ($curv = 0.664 \pm 0.21$) was significantly higher ($p < 0.001$, Fig. 3c) than that of SLS ($curv = 0.267 \pm 0.076$). The passive stress–strain relationships of both groups are displayed in Fig. 4. Both curves were characterized by a course that resembles an exponential increase of stress with muscle length. No statistically significant differences were found between the two groups for p_{pass} .

Discussion

To our knowledge, there has not been a systematic study that examined the influence of layer separation on smooth muscle strip properties. Therefore, the present study performed in vitro uniaxial tensile experiments on tissue samples from the fundus of the porcine stomach to characterize the FLR and FVR of WMS and SLS. We found apparent differences

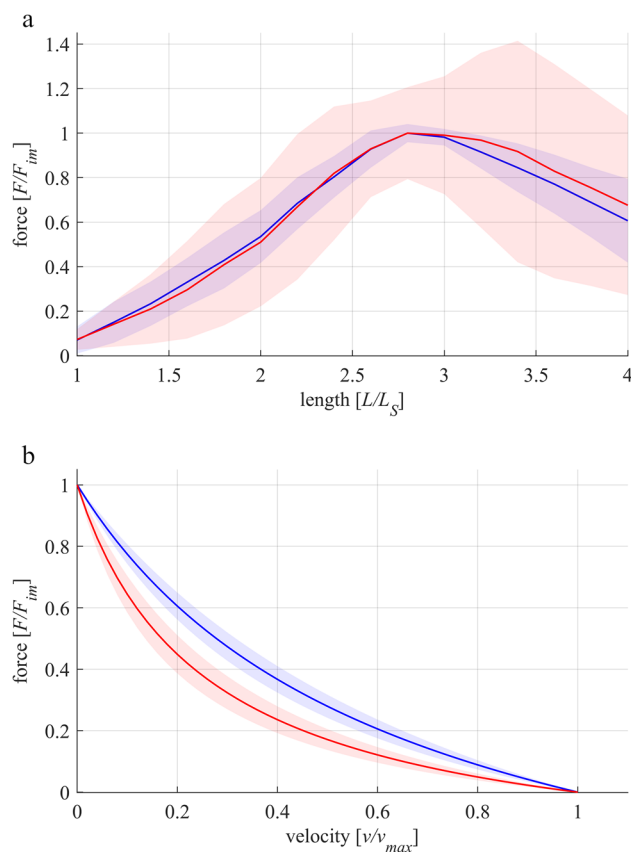


Fig. 2 Active muscle properties of whole-muscle strips (WMS, blue color) and isolated layer strips (SLS, red color). The solid curves and light-shaded areas indicate mean values and standard deviations, respectively. **a** Active force–length relationship. Force and length are normalized to maximum isometric force (F_{im}) and slack length (L_S), respectively. Isometric force–length measurements comprise $n = 10$ tissue samples for whole-muscle strips and $n = 9$ samples for isolated layer strips. **b** Force–velocity relationship. Velocity and force values are normalized to maximum shortening velocity (v_{max}) and F_{im} , respectively. Based on a series of 6 isotonic contractions, the force–velocity curves of $n = 7$ tissue samples were fitted using the typical Hill equation [20, 43]

in muscle properties determined from shortening contractions, such as in the parameters v_{max} and $curv$. In contrast, there was a negligible influence of layer separation on the normalized FLR parameters determined from isometric

Table 2 Influence of layer separation on optimal length (L_0), the width of ascending (w_{asc}), and descending limb (w_{desc}) of the force–length relationship and passive stress (p_{pass}) at L_0 . n.s., not significant

Sample	L_0 (L/L_S)	w_{asc} (L/L_0)	w_{desc} (L/L_0)	p_{pass} (kPa)
Whole-muscle strips	2.86 ± 2.32	0.67 ± 0.07	1.29 ± 0.98	20.6 ± 13.6
Separated layer strips	2.97 ± 4.29	0.63 ± 0.05	0.87 ± 0.58	20.3 ± 8.2
p	0.461 (n.s.)	0.203 (n.s.)	0.273 (n.s.)	0.944 (n.s.)

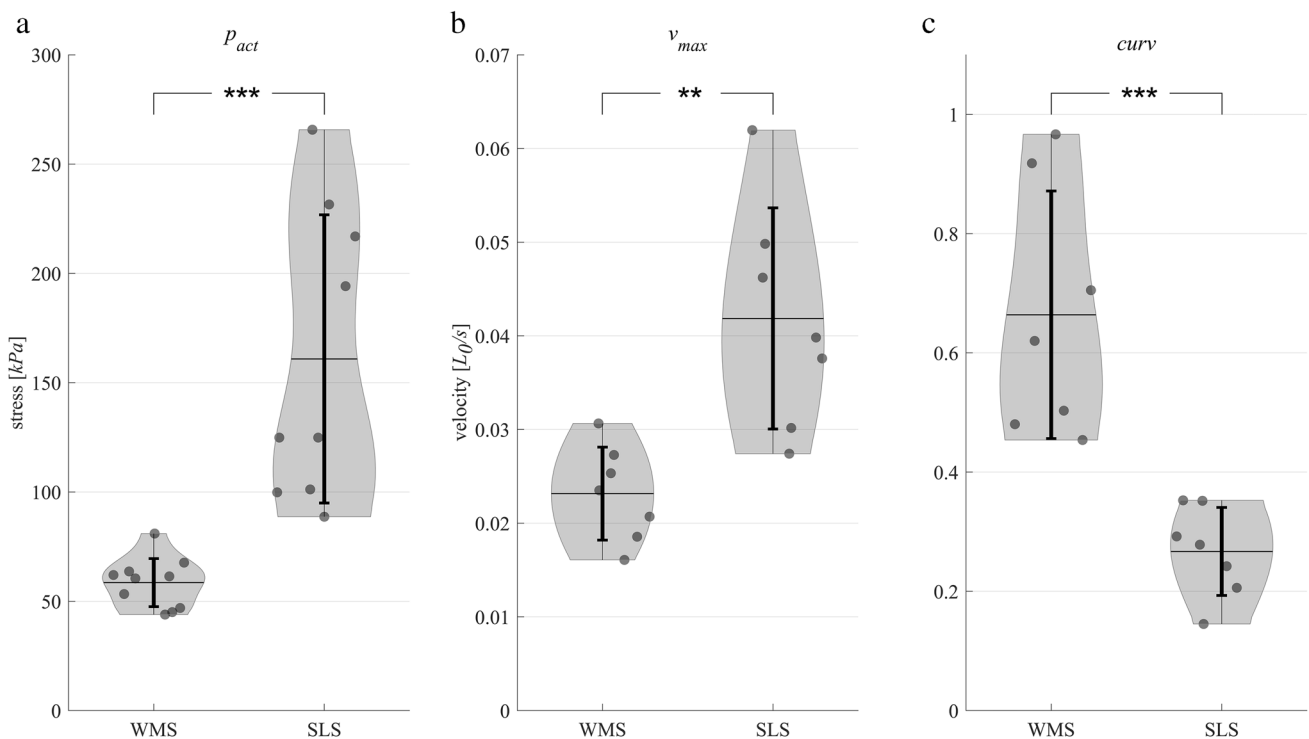


Fig. 3 **a** Influence of layer separation on maximum active isometric stress (p_{act}), **b** maximum shortening velocity (v_{max}), and **c** *curv* factor of the force–velocity relationship (FVR). For whole-muscle strips (WMS) and separated layer strips (SLS), mean values \pm standard deviations are displayed by the black horizontal line and the verti-

cal error bars, respectively. The transparent black markers indicate the individual data points. The shaded area (violin plot [21]) illustrates the distribution of the data. Brackets and asterisks (*) mark significant differences. Significance levels are marked as * $p < 0.01$ and * * * $p < 0.001$

contractions. These results are relevant for the determination of realistic muscle parameters, which are required in muscle models. Moreover, the results presented can be used

to check which parameters in the existing data are influenced by the interaction of multiple muscle layers.

Porcine smooth muscle properties—comparison with the literature

The average p_{act} of 160.9 ± 66.5 kPa generated by separated layer strips can be considered as the pure smooth muscle stress. Histological analyses yielded negligible amount of collagen in the circumferential muscle layer; see Fig. 1c. Observed p_{act} values are in agreement with stress values smooth muscles typically generate [8, 18, 47, 54]. The FLR displayed the typical bell shape of smooth, skeletal, and cardiac muscles. The extrapolated range, at which the muscle produced forces (0.35 to $2.08 L_0$), is similar to examined values of other studies on smooth muscles, which lie between 0.13 and $0.38 L_0$ [8, 28, 30, 36, 48, 49, 54, 60] and 1.82 and $2.17 L_0$ [8, 30, 36, 44, 49, 60]. The average v_{max} of $0.023 \pm 0.003 L_0/s$ and $0.042 \pm 0.012 L_0/s$ of WMS and SLS, respectively, are rather low, but within the range of reported values between 0.016 and $0.6 L_0/s$ of visceral smooth muscles [2, 3, 8, 16, 26–32, 34, 38, 39, 49, 55, 56]. The mean *curv* of 0.664 ± 0.21 and 0.267 ± 0.076 of WMS and SLS, respectively, are in agreement with values of 0.1–0.8 found

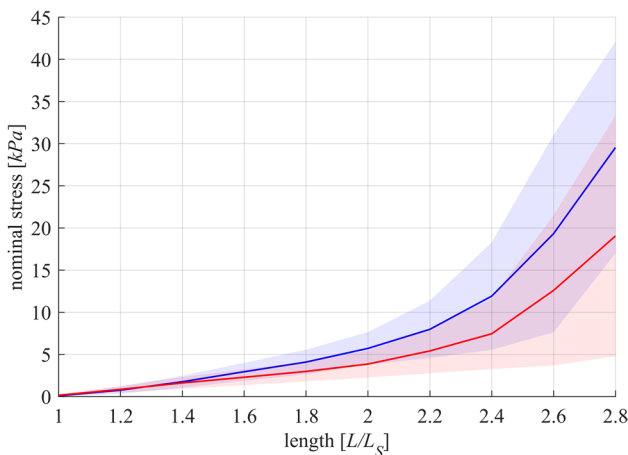


Fig. 4 Passive stress-length relationship of whole-muscle strips (blue) and separated layer strips (red). Force is divided by the cross-sectional area (CSA) of the strip at slack length (L_s) to obtain nominal stress. Passive stresses are measured right before activation on each length from isometric experiments. The solid curves and light-shaded areas indicate mean values and standard deviations, respectively

in smooth [2, 8, 16, 26, 27, 29–31, 34, 37–39, 47–49, 55] and skeletal muscles [43]. The mean p_{pass} of 20.6 ± 13.6 kPa of WMS at L_0 amount to about 35% of their average p_{act} (58.5 ± 11.5 kPa), which are in accordance with findings of previous studies on smooth muscles [16, 30, 49].

Influence of layer separation on smooth muscle properties

The separation of the circumferential smooth muscle layer affected the shortening characteristics of the examined tissue strips, as WMS displayed lower v_{max} and higher *curv* than SLS (Fig. 3b, c). WMS consisted of the circumferential and the longitudinal muscle layers, which were oriented in the lengthwise (e_{circ}) and transversal directions (e_{long}) of the strip, respectively (Fig. 5a). The two layers may be regarded as isolated, individual muscle layer strips. The muscle fibers of the longitudinal layer strip run along its narrow side (Fig. 5b, black arrow), whereas the muscle fibers of the circumferential layer strip run along its lengthwise side (Fig. 5c, black arrow). During isotonic contractions,

the circumferential layer shortens along the lengthwise axis of the strip (Fig. 5c, red arrow), while simultaneously the longitudinal layer shortens in the transverse direction of the strip (Fig. 5b, red arrows). The transverse shortening of the longitudinal layer causes a narrowing of the strip, which causes the strip to lengthen due to expected volume constancy of the muscle tissue. This lengthening is directed opposite the shortening of the circumferential muscle layer. Similar to myofascial force transmissions in skeletal muscles [22, 61], force transmission occurs between the neighboring smooth muscle layers. The lengthening of the longitudinal layer counteracts the concentric contraction of WMS, reducing its shortening velocity. As SLS does not contain the longitudinal layer, this effect does not apply, and the shortening velocity of SLS is not reduced. Therefore, SLS exhibited higher v_{max} than WMS (Fig. 3b). The shortening velocity of WMS was reduced more markedly compared to SLS at concentric contractions against low relative forces (high velocities) (Fig. 6).

During isometric contractions ($v=0$), no or negligible change in WMS strip length is expected. Due to volume

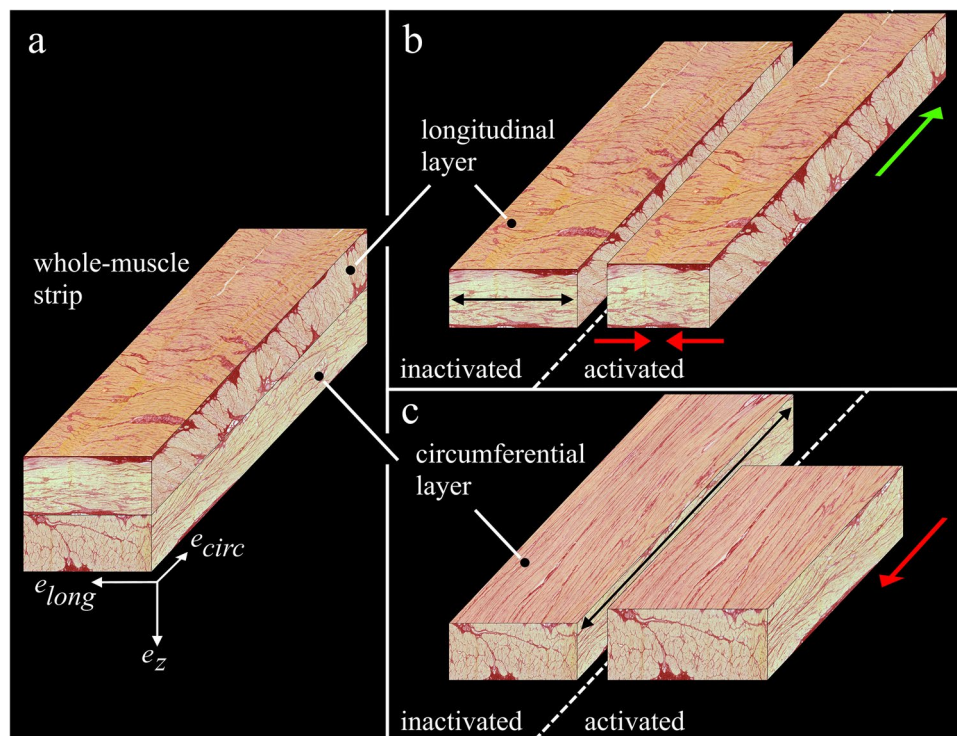


Fig. 5 Schematic reconstruction of whole-muscle strips from the porcine stomach during concentric contractions in uniaxial experiments. Strip representation is based on perpendicular histological examinations with Picrosirius Red staining protocol. **a** Whole-muscle strips were cut from the fundus (Fig. 1) lengthwise to the circumferential smooth muscle layer. They consisted of the outer longitudinal layer **b** and the inner circumferential layer **c**. When activated, both layers contracted concentrically along their muscle fiber direction (black

arrows in **b** and **c**). While the circumferential layer shortened lengthwise (**c**, red arrow), the longitudinal layer shortened transversally (**b**, red arrows). Due to volume constancy, the narrowing of the longitudinal layer prompted its simultaneous lengthening (green arrow). Through force transmission between the layers, this lengthening counteracted the shortening of the circumferential layer during the concentric contraction. Consequently, the shortening velocity was decreased in WMS

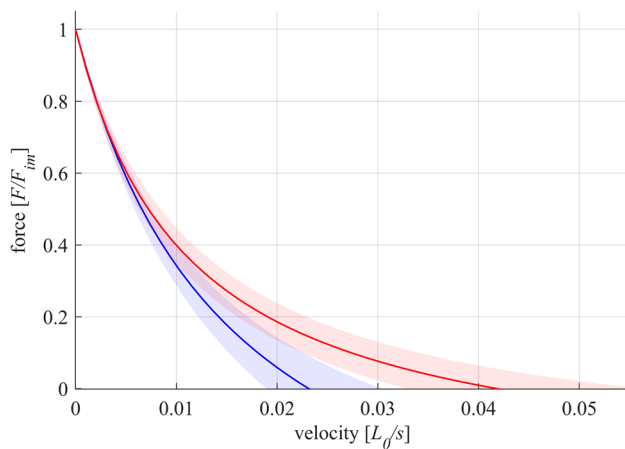


Fig. 6 Force–velocity relationship of whole-muscle strips (blue) and separated layer strips (red). Velocity and force values are normalized to optimum muscle length (L_0) and maximum isometric force (F_{im}), respectively. Based on a series of 6 isotonic contractions, the force–velocity curves of $n=7$ tissue samples were fitted using the typical Hill equation [20, 43]

constancy, this would result in no or negligible lengthening of the longitudinal layer and thus no or negligible counteracting forces of the longitudinal layer during isometric contractions. Counteracting forces of the longitudinal layer might decrease with decreasing velocity due to velocity-dependent viscoelastic properties of muscle tissue [59] and velocity-dependent damping properties of the FVR.

For the comparison of isometric contractions, the FLR was determined. As a result, the layer separation did not affect the shape of the FLR. However, the p_{act} was higher in SLS than that in WMS. While both groups consisted predominantly of muscle tissue, the longitudinal layer of the WMS did not generate tensile forces along the measuring force axis during isometric contractions due to the orientation of its muscle fibers in the transversal direction. Therefore, the active stress of WMS was lower due to the higher CSA of the WMS strip. Nevertheless, it remains a question whether the pure muscle stresses of the SLS and the WMS were different if the WMS force will be normalized by the CSA of only the tensile force-generating muscle tissue, i.e., its circumferential layer. However, for a valid analysis of such a parameter, determining CSA of both WMS muscle layers by histological examinations of all tested samples would be necessary, which was not performed in the present study.

The p_{pass} and the course of the nominal stress with increasing length did not differ between WMS and SLS (Table 2). This suggests an isotropic passive behavior of the smooth muscle tissue in the gastric fundus, agreeing with observations of studies that conducted biaxial experiments on tissue strips from this region [5, 6].

Relevance for studies on smooth muscle strips

It was shown that the examined muscle properties through uniaxial experiments are dependent on whether the muscle layers of smooth muscle strips are separated or not. From a physiological point of view, it would be preferable to separate the muscle layers, so smooth muscle properties are not influenced by such side effects. However, whole-muscle tissue strips represent more realistic samples for the organ wall in vivo, and hence may be more suitable for the three-dimensional modeling of organs. Furthermore, depending on the organ, or the animal from which the smooth muscle strips are harvested, it may not be possible to separate the muscle layers. For example, some regions of the bladder wall do not contain clearly separate muscle layers but rather multiple, differently oriented muscle fibers [33]. Studies on the stomach of guinea pigs [34] or the intestine of rabbits [13] report difficulties in separating the muscle layers, as this was not possible without potentially damaging the tissue. In this case, biaxial tension testing [14, 33, 52] of muscle tissue is recommended.

In sum, uniaxial experiments are a valid method to determine smooth muscle properties, especially if separated muscle layers were used. However, when conducting experiments on strips with multiple muscle layers, the effect of a transversal shortening needs to be considered and discussed.

Conclusion

The present study examined the influence of layer separation on the muscle properties of smooth muscle strips from the porcine stomach. SLS displayed higher v_{max} than WMS, as the contraction of the longitudinal layer of the WMS with its transversally oriented muscle fibers affected the shortening velocity. This effect is weaker with decreasing shortening velocity, which results in a lesser curvature (higher *curv* parameter) of the force–velocity relation of WMS compared to SLS. The FLR showed no differences in shape between the groups. However, SLS generated a higher p_{act} than WMS. This was due to higher CSA of WMS compared to SLS with the same amount of circumferential muscle layer tissue in WMS and SLS generating force in the direction of the force-measuring axis. The results of this study show that the determination of smooth muscle properties through uniaxial experiments may depend on whether the muscle layers are separated or not.

Abbreviations CSA: Cross-sectional area; *curv*: Curvature factor; F_{im} : Maximum isometric muscle force; FLR: Force–length relationship; FVR: Force–velocity relationship; L_0 : Optimum muscle length associated with F_{im} ; L_S : Slack length; p_{act} : Maximum active stress at L_0 ; p_{pass} : Passive stress at L_0 ; SLS: Separated layer strips; v_{max} : Maximum shortening velocity; w_{asc} : Width of the ascending limb; w_{desc} : Width of the descending limb; WMS: Whole-muscle strips

Author contribution Mischa Borsdorf: wrote the paper, conducted the experiments, and analyzed the data. Markus Böl: review and editing, coordinated the study. Tobias Siebert: designed and coordinated the study, wrote the paper.

Funding Open Access funding enabled and organized by Projekt DEAL. This work was funded by the Deutsche Forschungsgemeinschaft (DFG) under Grants SI 841/12–1 and BO 3091/18–1.

Data availability The datasets generated during and/or analysed during the current study are available from the corresponding author on reasonable request.

Declarations

Ethics approval The study was exempted from ethical committee review according to the National Regulations (German Animal Welfare Act) as porcine stomach smooth muscle tissue was obtained from a slaughterhouse immediately after animal sacrifice.

Conflict of interest The authors declare no competing interest.

Open Access This article is licensed under a Creative Commons Attribution 4.0 International License, which permits use, sharing, adaptation, distribution and reproduction in any medium or format, as long as you give appropriate credit to the original author(s) and the source, provide a link to the Creative Commons licence, and indicate if changes were made. The images or other third party material in this article are included in the article's Creative Commons licence, unless indicated otherwise in a credit line to the material. If material is not included in the article's Creative Commons licence and your intended use is not permitted by statutory regulation or exceeds the permitted use, you will need to obtain permission directly from the copyright holder. To view a copy of this licence, visit <http://creativecommons.org/licenses/by/4.0/>.

References

- An SS, Bai TR, Bates JHT et al (2007) Airway smooth muscle dynamics: a common pathway of airway obstruction in asthma. *Eur Respir J* 29:834–860. <https://doi.org/10.1183/09031936.00112606>
- Arner A (1982) Mechanical characteristics of chemically skinned guinea-pig taenia coli. *Pflüger's Arch - Eur J Physiol* 395:277–284. <https://doi.org/10.1007/BF00580790>
- Arner A, Hellstrand P (1985) Effects of calcium and substrate on force-velocity relation and energy turnover in skinned smooth muscle of the guinea-pig. *J Physiol* 360:347–365. <https://doi.org/10.1113/jphysiol.1985.sp015621>
- Arner A, Mattiasson A, Radziszewski P, Uvelius B (1998) Shortening velocity is different in longitudinal and circular muscle layers of the rabbit urethra. *Urol Res* 26:423–426. <https://doi.org/10.1007/s002400050080>
- Aydin RC, Brandstaeter S, Braeu FA, Steigenberger M, Marcus RP, Nikolaou K, Notohamiprodjo M, Cyron CJ (2017) Experimental characterization of the biaxial mechanical properties of porcine gastric tissue. *J Mech Behav Biomed Mater* 74:499–506. <https://doi.org/10.1016/j.jmbbm.2017.07.028>
- Bauer M, Morales-Orcajo E, Klemm L, Seydewitz R, Fiebach V, Siebert T, Böl M (2020) Biomechanical and microstructural characterisation of the porcine stomach wall: location- and layer-dependent investigations. *Acta Biomater* 102:83–99. <https://doi.org/10.1016/j.actbio.2019.11.038>
- Biancani P, Zabinski M, Kerstein M, Behar J (1982) Lower esophageal sphincter mechanics: anatomic and physiologic relationships of the esophagogastric junction of cat. *Gastroenterology* 82:468–475. [https://doi.org/10.1016/S0016-5085\(82\)80395-8](https://doi.org/10.1016/S0016-5085(82)80395-8)
- Borsdorf M, Tomalka A, Stutzig N, Morales-Orcajo E, Böl M, Siebert T (2019) Locational and directional dependencies of smooth muscle properties in pig urinary bladder. *Front Physiol* 10:63. <https://doi.org/10.3389/fphys.2019.00063>
- Brenner B (1983) Technique for stabilizing the striation pattern in maximally calcium-activated skinned rabbit psoas fibers. *Biophys J* 41:99–102. [https://doi.org/10.1016/S0006-3495\(83\)84411-7](https://doi.org/10.1016/S0006-3495(83)84411-7)
- Chen Y, Wang H, Li H, Liu S (2018) Long-pulse gastric electrical stimulation repairs interstitial cells of cajal and smooth muscle cells in the gastric antrum of diabetic rats. *Gastroenterol Res Pract*. <https://doi.org/10.1155/2018/6309157>
- Davis MJ, Davidson J (2002) Force-velocity relationship of myogenically active arterioles. *Am J Physiol* 282:H165–H174. <https://doi.org/10.1152/ajpheart.2002.282.1.h165>
- Davis MJ, Gore RW (1989) Length-tension relationship of vascular smooth muscle in single arterioles. *Am J Physiol* 256:H630–H640. <https://doi.org/10.1152/ajpheart.1989.256.3.h630>
- Elbrønd H, Tøttrup A, Forman A (1991) Mechanical properties of isolated smooth muscle from rabbit sphincter of oddi and duodenum. *Scand J Gastroenterol* 26:289–294. <https://doi.org/10.3109/00365529109025044>
- Gloeckner DC, Sacks MS, Fraser MO, Somogyi GT, De Groat WC, Chancellor MB (2002) Passive biaxial mechanical properties of the rat bladder wall after spinal cord injury. *J Urol* 167:2247–2252. <https://doi.org/10.1097/00005392-200205000-00080>
- Gordon AM, Huxley AF, Julian FJ (1966) The variation in isometric tension with sarcomere length in vertebrate muscle fibres. *J Physiol* 184(170–192):5921536
- Gordon AR, Siegman MJ (1971) Mechanical properties of smooth muscle. I. Length-tension and force-velocity relations. *Am J Physiol* 221:1243–1249. <https://doi.org/10.1152/ajplegacy.1971.221.5.1243>
- Griffiths DJ, van Mastriigt R, van Duyl WA, Coolsaet BLRA (1979) Active mechanical properties of the smooth muscle of the urinary bladder. *Med Biol Eng Comput* 17:281–290. <https://doi.org/10.1007/BF02443812>
- Harris DE, Warshaw DM (1991) Length vs. active force relationship in single isolated smooth muscle cells. *Am J Physiol* 260:C1104–C1112. <https://doi.org/10.1152/ajpcell.1991.260.5.c1104>
- Herlihy JT, Murphy RA (1973) Length-tension relationship of smooth muscle of the hog carotid artery. *Circ Res* 33:275–283. <https://doi.org/10.1161/01.RES.33.3.275>
- Hill AV (1938) The heat of shortening and the dynamic constants of muscle. *Proc R Soc B Biol Sci* 126:136–195. <https://doi.org/10.1098/rspb.1938.0050>
- Hintze JL, Nelson RD (1998) Violin plots: a box plot-density trace synergism. *Statistical Computing And Graphics*. *Source Am Stat* 52:181–184
- Huijing PA, Baan GC (2003) Myofascial force transmission: muscle relative position and length determine agonist and synergist muscle force. *J Appl Physiol* 94:1092–1107. <https://doi.org/10.1152/japplphysiol.00173.2002>
- Klemm L, Seydewitz R, Borsdorf M, Siebert T, Böl M (2020) On a coupled electro-chemomechanical model of gastric smooth muscle contraction. *Acta Biomater* 109:163–181. <https://doi.org/10.1016/j.actbio.2020.04.007>
- Liu LWC, Thuneberg L, Huizinga JD (1994) Selective lesioning of interstitial cells of Cajal by methylene blue and light leads to loss of slow waves. *Am J Physiol* 266:G485–G496. <https://doi.org/10.1152/ajpgi.1994.266.3.g485>
- Longhurst PA, Kang J, Wein AJ, Levin RM (1990) Comparative length-tension relationship of urinary bladder strips from

- hamsters, rats, guinea-pigs, rabbits and cats. *Pharmacology* 96A:221–225. [https://doi.org/10.1016/0300-9629\(90\)90069-5](https://doi.org/10.1016/0300-9629(90)90069-5)
26. Lowy J, Mulvany MJ (1973) Mechanical properties of guinea pig taenia coli muscles. *Acta Physiol Scand* 88:123–136. <https://doi.org/10.1111/j.1748-1716.1973.tb05439.x>
 27. Malmqvist U, Arner A (1991) Correlation between isoform composition of the 17 kDa myosin light chain and maximal shortening velocity in smooth muscle. *Pflüger's Arch - Eur J Physiol* 418:523–530. <https://doi.org/10.1007/BF00370566>
 28. Malmqvist U, Arner A, Uvelius B (1991) Mechanics and Ca²⁺-sensitivity of human detrusor muscle bundles studied in vitro. *Acta Physiol Scand* 143:373–380. <https://doi.org/10.1111/j.1748-1716.1991.tb09248.x>
 29. Mashima H, Okada T, Okuyama H (1979) Dynamics of contraction in the guinea pig taenia coli. *Jpn J Physiol* 29:85–98. <https://doi.org/10.2170/jjphysiol.29.85>
 30. Menzel R, Böhl M, Siebert T (2017) Importance of contraction history on muscle force of porcine urinary bladder smooth muscle. *Int Urol Nephrol* 49:205–214. <https://doi.org/10.1007/s11255-016-1482-x>
 31. Meiss RA (1971) Some mechanical properties of cat intestinal muscle. *Am J Physiol* 220:2000–2007. <https://doi.org/10.1152/ajplegacy.1971.220.6.2000>
 32. Minekus J, van Mastrigt R (2001) Length dependence of the contractility of pig detrusor smooth muscle fibres. *Urol Res* 29:126–133. <https://doi.org/10.1007/s002400000168>
 33. Morales-Orcajo E, Siebert T, Böhl M (2018) Location-dependent correlation between tissue structure and the mechanical behaviour of the urinary bladder. *Acta Biomater* 75:263–278. <https://doi.org/10.1016/j.actbio.2018.05.014>
 34. Moriya M, Miyazaki E (1985) Force-velocity characteristics of stomach muscle: a comparison between longitudinal and circular muscle strips. *Comp Biochem Physiol* 81A:531–537. [https://doi.org/10.1016/0300-9629\(85\)91021-7](https://doi.org/10.1016/0300-9629(85)91021-7)
 35. Muinuddin A, Shuwen XUE, Diamant NE (2001) Regional differences in the response of feline esophageal smooth muscle to stretch and cholinergic stimulation. *Am J Physiol* 281:G1460–G1467. <https://doi.org/10.1152/ajpgi.2001.281.6.g1460>
 36. Mulvany MJ, Warshaw DM (1979) The active tension-length curve of vascular smooth muscle related to its cellular components. *J Gen Physiol* 74:85–104. <https://doi.org/10.1085/jgp.74.1.85>
 37. Peiper U, Laven R, Ehl M (1975) Force velocity relationships in vascular smooth muscle. The influence of temperature. *Pflüger's Arch - Eur J Physiol* 356:33–45. <https://doi.org/10.1007/BF00583519>
 38. Pel JJM, van Asselt E, van Mastrigt R (2005) Contractile properties of inner and outer smooth muscle bundles from pig urinary detrusor. *Urol Res* 33:23–30. <https://doi.org/10.1007/s00240-003-0371-9>
 39. Pel JJM, van Asselt E, van Mastrigt R (2006) Contractile properties of the proximal urethra and bladder in female pig: morphology and function. *Neurourol Urodyn* 25:70–77. <https://doi.org/10.1002/nau.20156>
 40. Sanders KM, Burke EP, Stevens RJ (1989) Effects of methylene blue on rhythmic activity and membrane potential in the canine proximal colon. *Am J Physiol* 256:G779–G784. <https://doi.org/10.1152/ajpgi.1989.256.4.g779>
 41. Sarriá R, Latorre R, Henroteaux M, Henroteaux N, Soria F, Pérez-Cuadrado E, López Albors O (2012) Morphometric study of the layers of the canine small intestine at five sampling sites. *Vet J* 192:498–502. <https://doi.org/10.1016/j.tvjl.2011.06.041>
 42. Seydewitz R, Menzel R, Siebert T, Böhl M (2017) Three-dimensional mechano-electrochemical model for smooth muscle contraction of the urinary bladder. *J Mech Behav Biomed Mater* 75:128–146. <https://doi.org/10.1016/j.jmbbm.2017.03.034>
 43. Siebert T, Leichsenring K, Rode C, Wick C, Stutzig N, Schubert H, Blickhan R, Böhl M (2015) Three-dimensional muscle architecture and comprehensive dynamic properties of rabbit gastrocnemius, plantaris and soleus: Input for simulation studies. *PLoS ONE* 10:e0130985. <https://doi.org/10.1371/journal.pone.0130985>
 44. Siegman MJ, Davidheiser S, Mooers SU, Butler TM (2013) Structural limits on force production and shortening of smooth muscle. *J Muscle Res Cell Motil* 34:43–60. <https://doi.org/10.1007/s10974-012-9333-6>
 45. Sjuve R, Haase H, Morano I, Uvelius B, Arner A (1996) Contraction kinetics and myosin isoform composition in smooth muscle from hypertrophied rat urinary bladder. *J Cell Biochem* 63:86–93. [https://doi.org/10.1002/\(SICI\)1097-4644\(199610\)63:1%3c86::AID-JCB7%3e3.0.CO;2-W](https://doi.org/10.1002/(SICI)1097-4644(199610)63:1%3c86::AID-JCB7%3e3.0.CO;2-W)
 46. Stållhand J, Holzapfel GA (2016) Length adaptation of smooth muscle contractile filaments in response to sustained activation. *J Theor Biol* 397:13–21. <https://doi.org/10.1016/j.jtbi.2016.02.028>
 47. Stephens NL (1985) Force-velocity constants in smooth muscle: afterload isotonic and quick-release methods. *Can J Physiol Pharmacol* 63:48–51. <https://doi.org/10.1139/y85-008>
 48. Stephens NL, Kroeger E, Mehta JA (1969) Force-velocity characteristics of airway smooth muscle. *J Appl Physiol* 26:685–692. <https://doi.org/10.1152/jappl.1969.26.6.685>
 49. Tomalka A, Borsdorf M, Böhl M, Siebert T (2017) Porcine stomach smooth muscle force depends on history-effects. *Front Physiol* 8:802. <https://doi.org/10.3389/fphys.2017.00802>
 50. Tomalka A, Röhrle O, Han JC, Pham T, Taberner AJ, Siebert T (2019) Extensive eccentric contractions in intact cardiac trabeculae: revealing compelling differences in contractile behaviour compared to skeletal muscles. *Proc R Soc B Biol Sci* 286:20190719. <https://doi.org/10.1098/rspb.2019.0719>
 51. Tøttrup A, Forman A, Uldbjerg N, Funch-Jensen P, Andersson KE (1990) Mechanical properties of isolated human esophageal smooth muscle. *Am J Physiol* 258:G338–G343. <https://doi.org/10.1152/ajpgi.1990.258.3.g338>
 52. Trostorf R, Morales-Orcajo E, Siebert T, Böhl M (2021) Location- and layer-dependent biomechanical and microstructural characterisation of the porcine urinary bladder wall. *J Mech Behav Biomed Mater* 115:104275. <https://doi.org/10.1016/j.jmbbm.2020.104275>
 53. Turner WH, Brading AF (1997) Smooth muscle of the bladder in the normal and the diseased state: pathophysiology, diagnosis and treatment. *Pharmacol Ther* 75:77–110. [https://doi.org/10.1016/S0163-7258\(97\)00038-7](https://doi.org/10.1016/S0163-7258(97)00038-7)
 54. Uvelius B (1976) Isometric and isotonic length-tension relations and variations in cell length in longitudinal smooth muscle from rabbit urinary bladder. *Acta Physiol Scand* 97:1–12. <https://doi.org/10.1111/j.1748-1716.1976.tb10230.x>
 55. Uvelius B (1977) Influence of muscle length on the force-velocity relation of K⁺-contractures in smooth muscle from rabbit urinary bladder. *Acta Physiol Scand* 101:270–277. <https://doi.org/10.1111/j.1748-1716.1977.tb06008.x>
 56. Uvelius B (1979) Shortening velocity, active force and homogeneity of contraction during electrically evoked twitches in smooth muscle from rabbit urinary bladder. *Acta Physiol Scand* 106:481–486. <https://doi.org/10.1111/j.1748-1716.1979.tb06429.x>
 57. van Mastrigt R (1988) The length dependence of the series elasticity of pig bladder smooth muscle. *J Muscle Res Cell Motil* 9:525–532. <https://doi.org/10.1007/BF01738757>
 58. van Mastrigt R, Glerum JJ (1985) Electrical stimulation of smooth muscle. *J Biomed Eng* 7:2–8. [https://doi.org/10.1016/0141-5425\(85\)90002-0](https://doi.org/10.1016/0141-5425(85)90002-0)

59. Van Looke M, Lyons CG, Simms CK (2008) Viscoelastic properties of passive skeletal muscle in compression: stress-relaxation behaviour and constitutive modelling. *J Biomech* 41:1555–1566. <https://doi.org/10.1016/j.jbiomech.2008.02.007>
60. Wingard CJ, Browne AK, Murphy RA (1995) Dependence of force on length at constant cross-bridge phosphorylation in the swine carotid media. *J Physiol* 488:729–739. <https://doi.org/10.1113/jphysiol.1995.sp021004>
61. Yucesoy CA (2010) Epimuscular myofascial force transmission implies novel principles for muscular mechanics. *Exerc Sport Sci Rev* 38:128–134. <https://doi.org/10.1097/JES.0b013e3181e372ef>

Publisher's note Springer Nature remains neutral with regard to jurisdictional claims in published maps and institutional affiliations.